

2000

# Centrifugal Compressor Multi-Mode Rotating Stall Control

E. C. Day  
*GE Aircraft Engines*

P. B. Lawless  
*Purdue University*

S. Fleeter  
*Purdue University*

Follow this and additional works at: <https://docs.lib.purdue.edu/icec>

---

Day, E. C.; Lawless, P. B.; and Fleeter, S., "Centrifugal Compressor Multi-Mode Rotating Stall Control" (2000). *International Compressor Engineering Conference*. Paper 1366.  
<https://docs.lib.purdue.edu/icec/1366>

This document has been made available through Purdue e-Pubs, a service of the Purdue University Libraries. Please contact [epubs@purdue.edu](mailto:epubs@purdue.edu) for additional information.

Complete proceedings may be acquired in print and on CD-ROM directly from the Ray W. Herrick Laboratories at <https://engineering.purdue.edu/Herrick/Events/orderlit.html>

# CENTRIFUGAL COMPRESSOR MULTI-MODE ROTATING STALL CONTROL

Elizabeth C. Day

GE Aircraft Engines  
Cincinnati, Ohio

Patrick B. Lawless

School of  
Mechanical Engineering  
Purdue University  
West Lafayette, Indiana

Sanford Fleeter

School of  
Mechanical Engineering  
Purdue University  
West Lafayette, Indiana

## ABSTRACT

To maintain stable operation, centrifugal compressors require a sufficient surge margin to avoid instabilities caused by small deviations in operating point or inlet conditions. When the operating point of a compressor nears the surge line, two unstable flow behaviors may exist – rotating stall and surge. The recent efforts in stall control have focused on the suppression of a single resonant mode, or stall cell pattern, to achieve range extension. A critical limitation of these techniques has been the eruption of higher order modes after the successful control of the first stall mode. To address this issue, experiments have been performed at Purdue University to investigate the feasibility of passive control of multi-mode rotating stall in centrifugal compressors. This is accomplished through experiments directed at characterizing the onset of rotating stall under the influence of a passive-dynamic multi-mode control scheme implemented in the Purdue Low Speed Centrifugal Compressor (PLCC).

## INTRODUCTION

When the operating point of a compressor nears the surge line, two unstable flow behaviors may exist – rotating stall and surge. Rotating stall is a non-axisymmetric disturbance that propagates around the annulus at some fraction of the wheel speed. The pressure rise falls to a reduced, albeit steady, value. In contrast, surge is an axisymmetric phenomenon which is characterized by a one-dimensional oscillation through the compression system. For a particular machine, rotating instabilities with different cell patterns and wave speeds may occur at different operating points. In both low speed and high speed centrifugal compressors, rotating stall is typically encountered when the machines are operated at speeds lower than the design speed. In high speed centrifugal compressors, there is some evidence that rotating stall may play an important role in the initiation of surge at design speed [1,2], although the evidence is less well substantiated than for multistage axial compressors. The operating point achieved in rotating stall is stable on a circumferentially averaged basis, albeit at reduced performance. While being subjected to rapid loading and unloading, the compressor blades can undergo dangerous structural excitation [3]. Because of disadvantages of operating a compressor in rotating stall, the capability to extend the stable operating range of a compressor, be it by either passive or active control techniques, is of great importance.

The path of a compressor to rotating stall is subject to some debate, with the two principle observed pathologies for axial compressors described by Day [4]. The instability may manifest itself as initially weak disturbances with a length scale on the order of machine circumference which grow in an operating region of low system damping. This so called “modal-wave” stalling behavior has been documented by a variety of researchers and also used as a basis for active control of the surge line in axial flow compressors [5]. Another approach to stall involves a strong separation on a length scale of blade spacing, with a corresponding strong perturbation in relative diffusion for the affected stream tube. Not only is the rapid, finite change in the local slope of the pressure rise characteristic highly destabilizing, but the flow path blockage can also drive the propagation of the separated zone as classically described by Emmons [6]

In radial flow compressors where the pressure rise is far less dependent on relative diffusion, the former, more gradual, modal wave type of stall pathology can be expected to be more common. Indeed, radial flow machines can exhibit propagating disturbances in the inducer region (inducer stall) without progressing to complete flow breakdown through the impeller. A low speed centrifugal research compressor at Purdue University

has been well documented to progress to stall via the growth of initially weak disturbances, or modal waves, which can be detected at the impeller inlet and exit as the compressor approaches the surge line [7]. These disturbances have been shown to be the result of small but finite perturbations in the impeller channel flow at approximately mid-chord, with the nearly sinusoidal nature of the signals at the inlet and exit of the impeller a result of the spatial decay of the higher, sub-resonant, harmonics of the disturbance[8,9].

Attempts to increase the stable operating range of compressors through aerodynamic control have been made using both passive and active methods. Classic passive techniques may employ changes in compressor geometry which result in extended surge margin through reduced endwall blockage or changes in incidence. Examples of such passive control methods include endwall treatments [10,11] and diffuser and inducer bleed slots [12]. Other more recent attempts at passive techniques achieve control by changing the dynamic characteristics of the compression system. In such passive-dynamic control schemes, there is no independent detection device, actuator, or control logic. Rather, the passive devices serve increase system damping at the resonant, or stall, frequency. Research efforts have also been directed toward active surge line control, which serves to increase the control authority (i.e. increase system damping) to levels higher than that achievable with passive techniques. Active control methods operate in a feedback mode, detecting a growing instability and introducing a countering fluid-dynamic disturbance. Active control techniques for rotating stall have been demonstrated in both low speed axial and centrifugal compressors [13, 14,15].

The recent efforts in stall control have focused on the suppression of a single resonant mode, or stall cell pattern, to achieve range extension. A critical limitation of these techniques has been the eruption of higher order modes after the successful control of the first stall mode. To address this issue, experiments have been performed at Purdue University to investigate the feasibility of passive control of multi-mode rotating stall in centrifugal compressors. This is accomplished through experiments directed at characterizing the onset of rotating stall under the influence of a passive-dynamic multi-mode control schemes implemented in the Purdue Low Speed Centrifugal Compressor.

## FACILITY AND INSTRUMENTATION

The Purdue Low Speed Centrifugal Compressor (PLCC), Figure 1, features a shrouded, mixed-flow impeller with 23 backswept blades. Following the impeller is a radial vaneless diffuser that can be configured with up to 30 cambered vanes. The compressor is driven by a 29.8 kW (40 Hp) induction motor. This motor produces a nominal operating speed of 1790 RPM, an impeller pass frequency of 28.9 Hz, and a blade pass frequency of 686.2 Hz.

Atmospheric air enters the compressor axially through the bell mouth opening and then passes through the impeller. At the impeller exit, flow travels through a curved vaneless space and exits into a parallel wall radial vaneless diffuser. Flow is then discharged into a scroll of square cross section. The exhaust is carried away by discharge piping that contains a sharp-edged orifice plate used for flow rate measurement. The piping is terminated by a gear-motor driven butterfly valve that is used to throttle the compressor.

The impeller is cast of aluminum and consists of 23 backswept blades. It is a mixed-flow design such that the flow is never turned to a completely radial direction. The velocity flow field at the impeller exit has components in the radial, tangential, and axial directions. The backsweep angle of the blades at the impeller exit is 51 degrees. A fiberglass shroud is attached to the tip of the impeller, eliminating the tip leakage flows in the endwall region of the impeller.

The diffuser section of the facility contains a curved vaneless space that smoothly turns the flow to the radial direction. A parallel wall radial vaneless diffuser follows the vaneless space. The cambered diffuser vanes have a NACA 4312 airfoil profile with a chord length of 16.5 cm (6.5 in.). The diffuser vanes are removable such that the facility can be configured with a maximum of 30 vanes, a reduced set of either 15 vanes, 10 vanes, or a vaneless configuration. The vanes are mounted on eccentric cams embedded in the diffuser endwall which allow the stagger angle as well as the vane leading edge radius to be varied.

## INSTRUMENTATION

The determination of the compressor performance is accomplished by monitoring pressures, flow rates, and temperature. The compressor exit pressure is measured with an OMEGA PX170 6.9 kPa (1 psi) differential pressure transducer. The exit plenum static pressure is assumed equal to the total pressure due to the large volume of the plenum and low plenum velocity. A hot film anemometer system measures the transient mass flow rate through the compressor. The system consists of a TSI model IFA-100 anemometer and a flat film model 1210-20 probe. The probe is centered in the discharge duct, eight pipe diameters, 325 cm (128 in.) upstream of an orifice plate. The orifice plate is used both to measure steady mass flow rate, with the film sensor then calibrated against the mass flow rate determined from the orifice plate. Assuming that the velocity profile in the exit duct does not change, instantaneous mass flow measurements are thus possible.

Additional transient instrumentation in the compressor is necessary to measure unsteady pressures in the inlet and diffuser sections. The compressor inlet is instrumented with an array of electret microphones that measures pressure unsteadiness. The array consists of 8 circumferentially spaced microphones mounted 1.8 cm (0.7 in.) in front of the leading edge of the impeller. An attenuator tube is installed between the endwall pressure port and the microphone. Thus, the low frequency rotating stall events are isolated from the high frequency blade-pass signal. The microphones were dynamically calibrated against a model 103A PCB microphone.

The simultaneous acquisition and digitization of time-varying signals is performed by National Instruments NB-A2000 analog to digital conversion boards. The boards are installed in an Apple Macintosh IIfx personal computer.

## EXPERIMENTAL TECHNIQUE

### Steady Performance

The quasi-steady performance of the compressor is characterized by measuring ambient pressure, exit plenum pressure, and mass flow rate as the compressor is slowly throttled into stall along a constant speed line. The compressor is throttled into stall by closing the butterfly valve at a constant rate. Data are sampled at 1600 Hz at the start of throttle movement and continues for 25 seconds through the stall event.

The stalling behavior of the compressor is characterized with the inlet unsteady pressures and the mass flow rate. Data are sampled at 2000 Hz while the compressor is throttled to stall. This is twenty times greater than the expected stall frequency and three times greater than blade pass frequency. For the throttling events in which the vane unsteady pressure transducers are sampled, data acquisition is triggered to obtain 15 seconds, 10 seconds pre-stall and 5 seconds post-stall. Compressor performance is expressed in term of the pressure rise coefficient ( $\Psi$ ) as a function of the flow coefficient ( $\phi$ ). The flow coefficient is defined as the ratio of the through flow velocity to the wheel speed at the compressor inlet,

$$\phi = \frac{\dot{m}}{\rho_{atm} A_i U_i}$$

where  $\dot{m}$  is the mass flow rate through the compressor,  $\rho_{atm}$  is ambient air density,  $A_i$  is the impeller inlet area, and  $U_i$  is the wheel speed at the mean impeller inlet radius. The pressure rise coefficient for the compressor is defined by

$$\Psi = \frac{P_{t,plenum} - P_{atm}}{\rho_{atm} U_i^2}$$

where  $P_{t,plenum}$  and  $P_{atm}$  represent the stagnation pressures in the plenum and atmospheric pressure respectively,  $\rho_{atm}$  is ambient air density, and  $U_i$  is the impeller wheel speed at the mean inlet radius.

### Stall Point Determination

The unsteady pressure signal used for the stall point analysis is sampled from the raw voltage of one electret microphone at the inlet of the compressor. As the compressor is throttled along a constant speed line, the unsteadiness is quantified by the standard deviation of the raw unfiltered unsteady pressures. As the stall event is initiated, the nonaxisymmetric rotating stall produces a large increase in the unsteady pressure. When the

variation of the unsteady pressure is charted versus the flow coefficient, the development of the compressor stall is evident. Thus, the flow coefficient at the moment of stall onset can clearly be identified.

### Rotating Stall Characterization

The rotating stall event is characterized by a spatially nonuniform pressure variation at the compressor inlet. The microphone array at the inlet measures the pressure unsteadiness. Static pressure taps on the outside diameter endwall of the inlet section connect the microphones to the compressor flow. As the compressor is throttled into rotating stall, the inlet microphones are simultaneously sampled at 2000 Hz. The frequency of the stall event is determined from a joint time-frequency analysis (i.e. waterfall plot). After performing the joint time-frequency analysis, events that occur at rotating stall frequencies are further isolated when the unsteady pressure signals are numerically band pass filtered, then are processed with a spatial Fourier transform to characterize the stall eruption and indicate any waveforms present. The resultant harmonics of this transform correspond to wave numbers or modes of sinusoidal distortions propagating around the compressor annulus and hence are indicative of rotating stall conditions. This procedure is described in detail by Day [16]

### Control System

The two degree-of-freedom Helmholtz resonators designed for the compressor mate with the diffuser as shown in Figure 2. The resonators are connected to ports between the diffuser vanes. A schematic of the devices are shown in Figure 3. Both chambers are comprised of 15.24 cm (6 inch) PVC pipe. The ends of the first chamber are closed with discs cut from 0.318 cm (0.125 in.) sheet PVC. A hole in each disc allows for the entrance of a runner. The first chamber is 11.43 cm (4.5 in.) in length, yielding a volume of 2080 cm<sup>3</sup>. The first chamber is connected to the second chamber by a second runner, 26.67 cm (10.5 in.) piece of 0.75 in. PVC pipe. The second runner enters the second chamber through another PVC sheet disc. The second chamber is 14.29 cm (5.625 in.) in length yielding a volume of 2600 cm<sup>3</sup>. As shown in Figure 3, a speaker can be mounted in the second chamber to provide active control, although this feature was not used in the current study.

The bandstop characteristic of the passive Helmholtz resonator can be plotted against frequency to show its effective bandwidth, shown in Figure 4. The Helmholtz frequencies occur at 23 and 57 Hz when the transmission coefficient decreases to zero. Geometric variables were chosen such that Helmholtz frequencies were near the first and second rotating stall mode frequencies of 24 and 54 Hz. The half power attenuation, or bandwidth, for the 24 Hz signal is 21 to 25 Hz. The bandwidth for the 54 Hz signal is 55 to 59 Hz. Experimental studies on the devices indicated the actual center band frequencies to be 19 and 58 Hz, and the performance was deemed acceptable for the experiments.

## RESULTS

### Baseline Stalling Behavior

The Purdue Low Speed Centrifugal Compressor was studied in its baseline configuration, which consists of 15 diffuser vanes at a 70° stagger. The compressor steady state performance both with and without the passive control devices is presented in Figure 5. In its baseline configuration with no passive control the compressor achieves a pressure coefficient of 1.96, and stalls at a flow coefficient of 0.316.

To initiate stall, the compressor was run at a constant design speed of 1790 rpm and the exit throttle slowly closed. The compressor stalling point was determined by observation of the standard deviation of the inlet microphone voltage. Figure 6 presents the standard deviation of the inlet microphone signal as a function of flow coefficient for nine separate stall events in the baseline configuration. The eruption of rotating stall in the compressor is indicated by the intense rise in the standard deviation. For these experiments a standard deviation of 0.25 was selected to define the stalling point of the compressor. Variations can be observed between the stalling events, therefore it was necessary to acquire many events and average the results. Twenty throttlings were taken for each compressor configuration that was studied.

To identify stall cell eruption, a spatial analysis was performed on the inlet microphone signals to identify the nature of onset of rotating stall. The magnitudes of the modes as a function of flow coefficient are presented as the baseline compressor is throttled into stall in Figure 7. The baseline configuration shows that the modes erupt in sequential order (i.e. 1,2,3). All three modes begin to rise at a flow coefficient of 0.325. The first mode (one cell stall-24 Hz) peaks at 0.23 kPa at a flow coefficient of 0.295 and ends its eruption at  $\phi = 0.28$ . The second

mode (two cell stall-54 Hz) peaks at 0.52 kPa at a flow coefficient of 0.27. The second mode diminishes at  $\phi = 0.22$ , and the third mode (three cell stall-83 Hz) peaks at 0.64 kPa. The third mode eruption is finally complete at  $\phi = 0.20$ . Since the breakdown of the compressor flow is complete at this point, regions of lower flow coefficients are not of interest.

#### Stalling Behavior with Passive Control

Figure 8 shows the mode magnitudes during throttle down with the passive control system activated. The first mode begins its rise at  $\phi = 0.33$  to 0.22 kPa. The second mode develops at  $\phi = 0.31$  and only rises to about half of the magnitude it has in the baseline configuration. The third mode increases at  $\phi = 0.33$  and rises to 0.70 kPa at  $\phi = 0.24$ , which is an increase of 0.07 kPa from its magnitude in the baseline configuration. During passive control, the first mode seems to remain the same as in the baseline case, while the second mode is greatly reduced in magnitude, and the third mode is slightly enhanced. The passive control, which is designed to control Modes 1 and 2, decreased only Mode 2 magnitude, however, the onset of stall, as indicated by the signal standard deviation, is delayed by  $\Delta\phi = 0.015$ . This  $\Delta\phi$  indicates that a change has occurred in way the compressor throttles to stall, not necessarily that the true stall point has changed.

Pre-stall behavior in the passive configuration is shown in Figures 9-11, where a comparison is made of the baseline (no control) versus the passive control case for each mode. Mode 1 experiences a similar precursory rise in magnitude is similar to the baseline, Figure 9, with only slight attenuation noted as the compressor begins to fall into a stall condition. In Figure 10, the strong attenuation of the second spatial mode is clearly shown. Corresponding to this attenuation, a strong amplification of the third mode occurs, as shown in Figure 11.

## DISCUSSION AND CONCLUSIONS

These experiments characterized the onset of rotating stall in the Purdue Centrifugal Compressor, with Helmholtz resonators tuned to two rotating stall frequencies connected to the vaned diffuser. The resonators were shown to affect the compressor's rotating stall behavior. The passive control extends the indicated stalling point from the baseline, no-control configuration. However, although the second mode magnitude is reduced by half during stall initiation, the first mode is only slightly affected. This result was not entirely unexpected, as previous studies focussed singularly on the first mode event showed that it is a fairly strong event and passive techniques provide limited control authority. As the control system is capable of active control through speakers mounted in the resonator cavities, attempts to further suppress this first mode without eliminating the successful passive attenuation of the second mode are currently underway.

It is interesting to note that as the second mode is suppressed, the third spatial mode takes on a larger role at the compressor stalls, limiting possible range extension. However, the third mode seems to set the limit on spatially coherent eruptions in the impeller of this machine, and thus further work directed at suppressing all three events would be of interest to determine the final destination of the stall trajectory.

## REFERENCES

1. Ffowcs Williams, J.E., Harper, M.F.L., and Allwright, D.J., 1992, "Active Stabilization of Compressor Instability and Surge in a Working Engine," *ASME Paper 92-GT-88*.
2. Oakes, W. C., Lawless, P.B., and Fleeter, S., 1996, "High Speed Centrifugal Compressor Surge Initiation Characterization," *AIAA Paper 96-2577*.
3. Haupt, U., Abdel-Hamid, A.N., Kaemmer, N., and Rautenberg, M., 1986, "Excitation of Blade Vibration by Flow Instability in Centrifugal Compressors," *ASME Paper 86-GT-283*.
4. Day, I.J., 1991, "Stall Inception in Axial Flow Compressors," *ASME Journal of Turbomachinery*, Vol. 115, No. 1, January, pp. 1-9.
5. Paduano, J., Epstein, A.H., Valavani, L., Longley, J.P., Greitzer, E.M., and Guenette, G.R., 1991, "Active Control of Rotating Stall in a Low Speed Axial Compressor," *ASME Paper 91-GT-88*.

6. Emmons, H.W., Pearson, C.E., and Grant, H.P., 1955, "Compressor Surge and Stall Propagation," *Transactions of the ASME*, Vol. 79, April, pp. 455-469
7. Lawless, P.B., and S. Fleeter, 1993, "Rotating Stall Acoustic Signature in a Low Speed Centrifugal Compressor Part II: Vaned Diffuser," *ASME Paper 93-GT-254*.
8. Oakes, W.C., Lawless, P.B., and S. Fleeter, 1995, "Characterization of the Behavior of a Centrifugal Compressor With Active Stall Control," *AIAA Paper 95-2484*.
9. Lawless, P.B., 1997 "Experimental Evaluation of Precursors to Centrifugal Compressor Stability," *ISABE Thirteenth International Symposium of Air Breathing Engines*.
10. Osborn, W.M., Lewis, G.W., Jr., and Heidelberg, L.J., 1971, "Effect of Several Porous Casing Treatments on Stall Limit and on Overall Performance of an Axial-Flow Compressor Rotor," *NASA TND-6537*
11. Moore, R.D., Kovich, G., and Blade, R.J., 1971, "Effect of Casing Treatment on Overall and Blade-Element Performance of a Compressor Rotor," *NASA TND-6538*.
12. Fisher, F.B., 1988, "Application of Map Width Enhancement Devices to Turbocharger Compressor Stages," *SAE Paper 880794*.
13. Day, I.J., 1991, "Active Suppression of Rotating Stall and Surge in Axial Compressors," *ASME Paper 91-GT-87*.
14. Lawless, P.B. and Fleeter, S., 1994, "Effect of Controlled Inlet Distortions on Rotating Stall Inception in a Low Speed Centrifugal Compressor," *AIAA Paper 94-2799*.
15. Trembl, B.J., 1997, "Passive and Active Control of Rotating Stall Onset in a Centrifugal Compressor," MS Thesis, Purdue University.
16. Day, E.C., 1999, "Active and Passive Multi-mode Control of Rotating Stall in a Centrifugal Compressor," MSME Thesis, Purdue University.

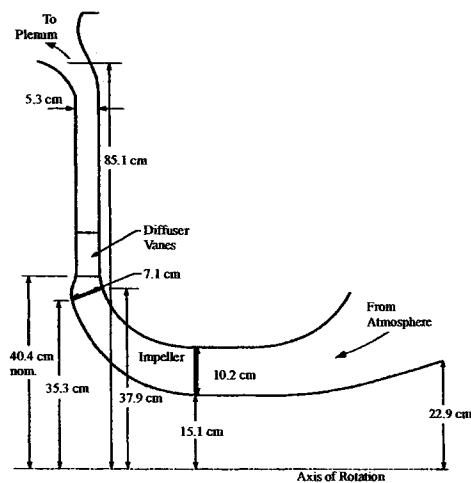


Figure 1. Purdue Low Speed Centrifugal Compressor

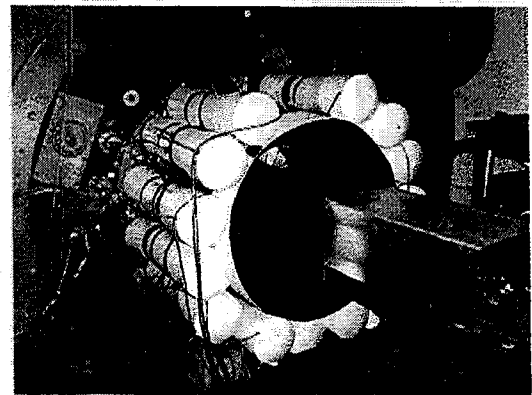


Figure 2. Compressor with Helmholtz resonators

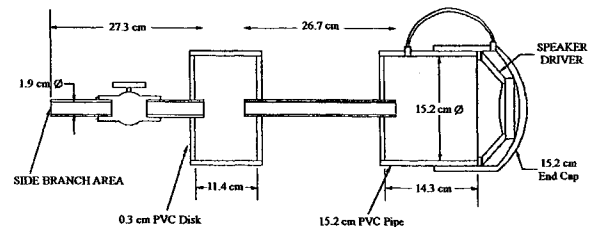


Figure 3. Second-order Helmholtz resonator

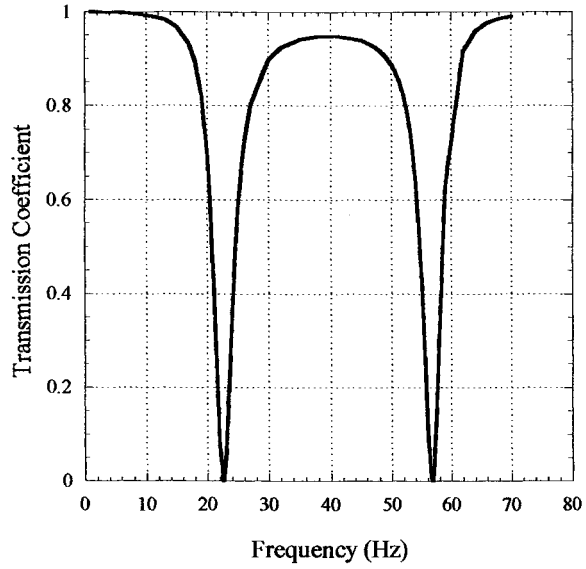


Figure 4. Resonator stop bands

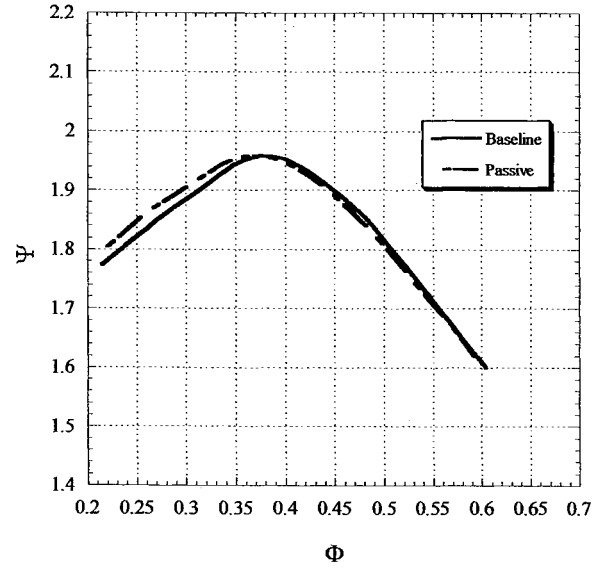


Figure 5. Compressor performance

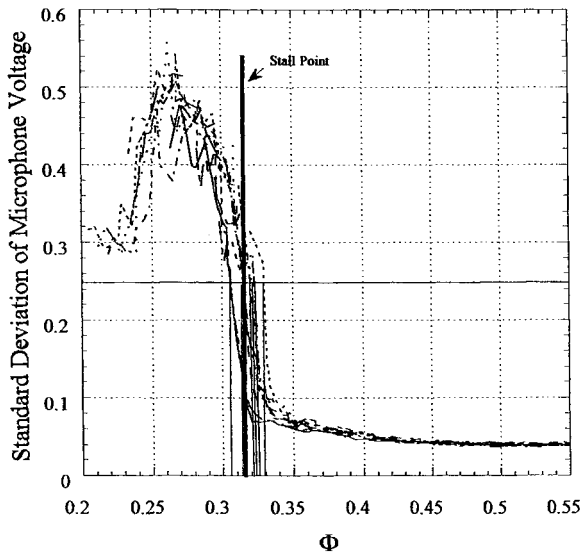


Figure 6. Determination of stall point

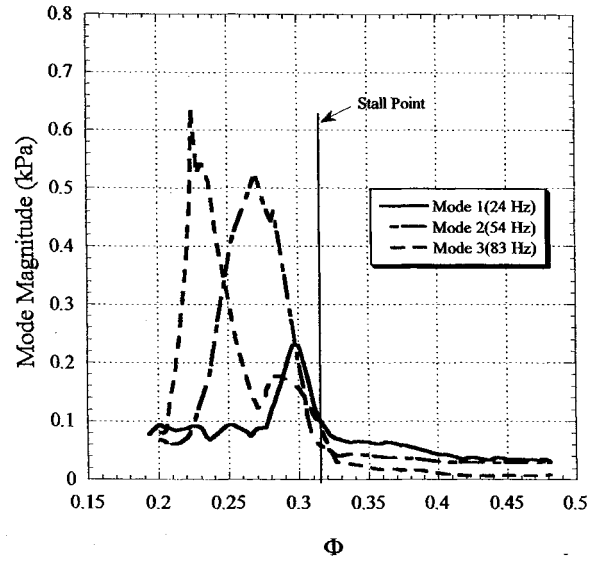


Figure 7. Baseline stalling behavior



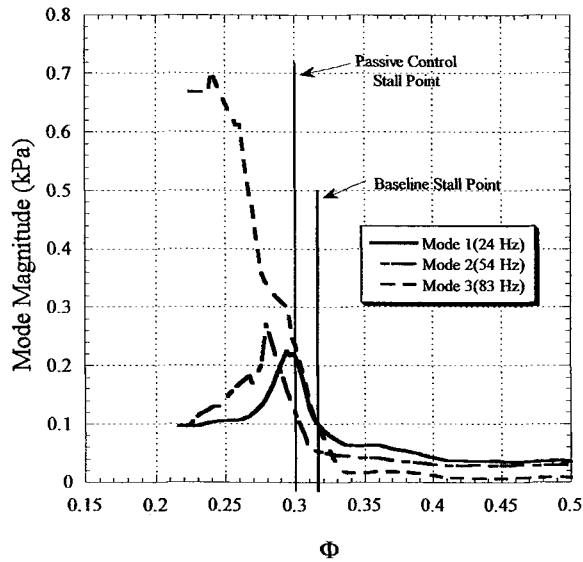


Figure 8. Stalling behavior with passive control

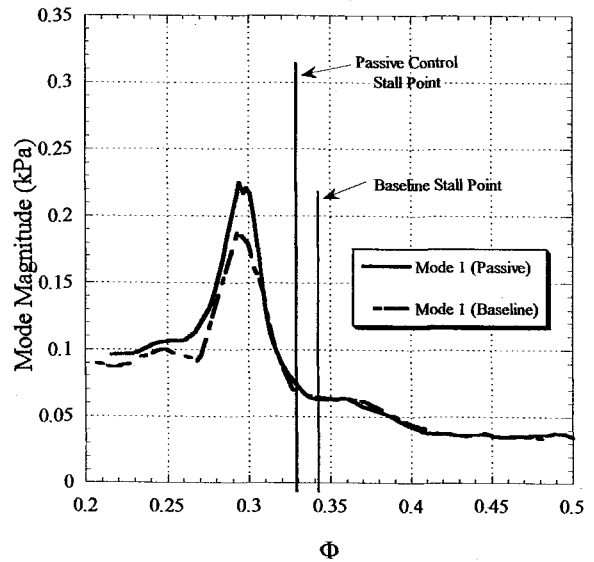


Figure 9. First mode comparison

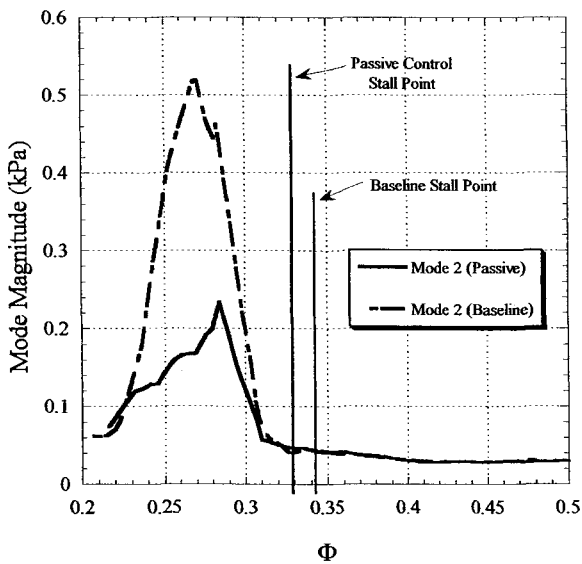


Figure 10. Second mode comparison

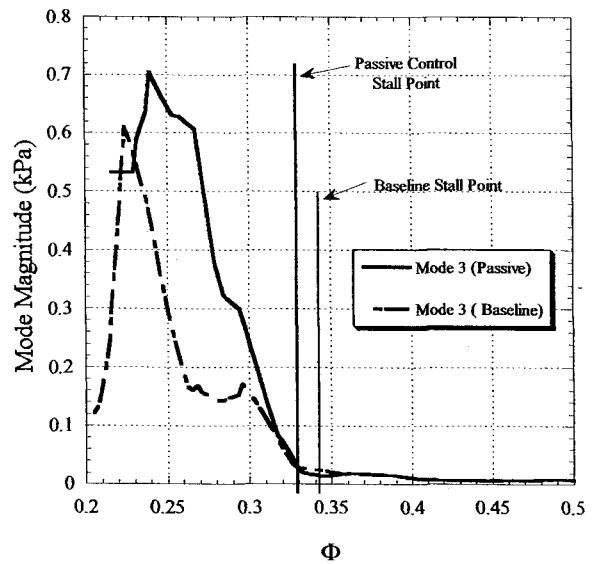


Figure 11. Third mode comparison